Supporting Information

Guest Induced Reversible ON-OFF Switching of Elastic Frustration in a 3D Spin Crossover Coordination Polymer with Room Temperature Hysteretic Behaviour

L. Piñeiro-López, F.-J. Valverde-Muñoz, E. Trzop, M. C. Muñoz, M. Seredyuk, J. Castells-Gil, I. da Silva, Carlos Martí-Gastaldo, E. Collet, J. A. Real.

Figure S1. IR spectrum of **1·PhNO$_2$** and **1** in the wave-length window 2000-1200 cm^{-1} emphasising the evolution of the characteristic asymmetric and symmetric stretching modes when moving from **1·PhNO$_2$** to **1** (vertical red lines indicate the position of both modes).

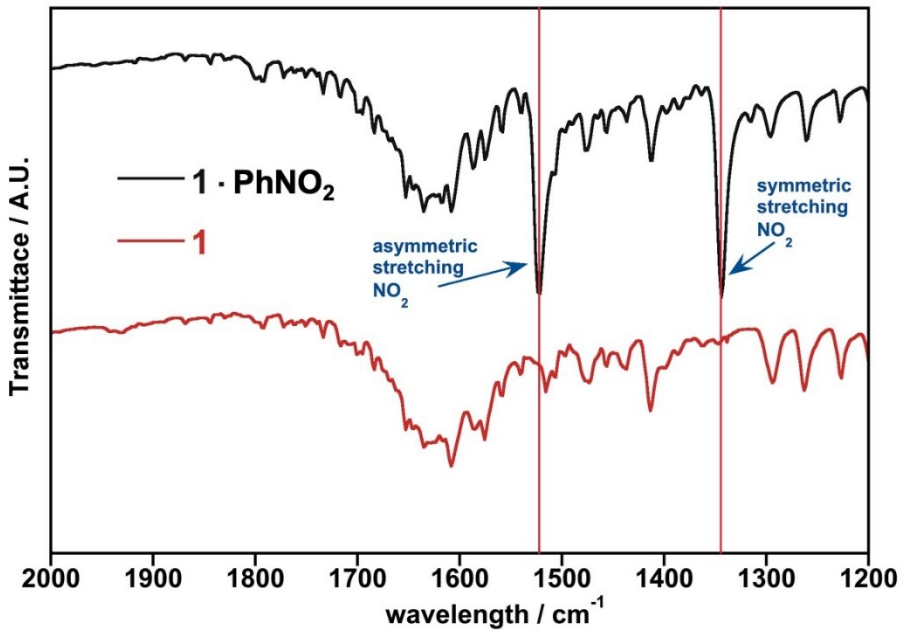

Figure S2. Thermogravimetric analysis of **1·PhNO$_2$**.

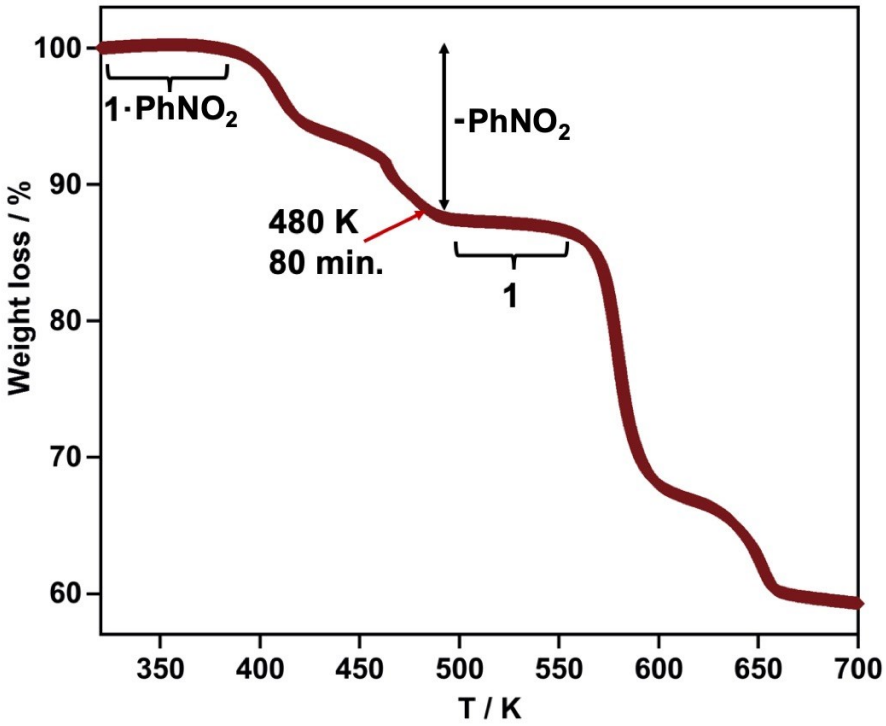

Figure S3. Thermal dependence of $\chi_M T$ for **1·PhNO$_2$** before desorption of $PhNO_2$ (left) and after re-adsorption of $PhNO_2$ (right) from the desorbed compound **1** (middle). Blue and red dots correspond to the cooling and heating modes, respectively.

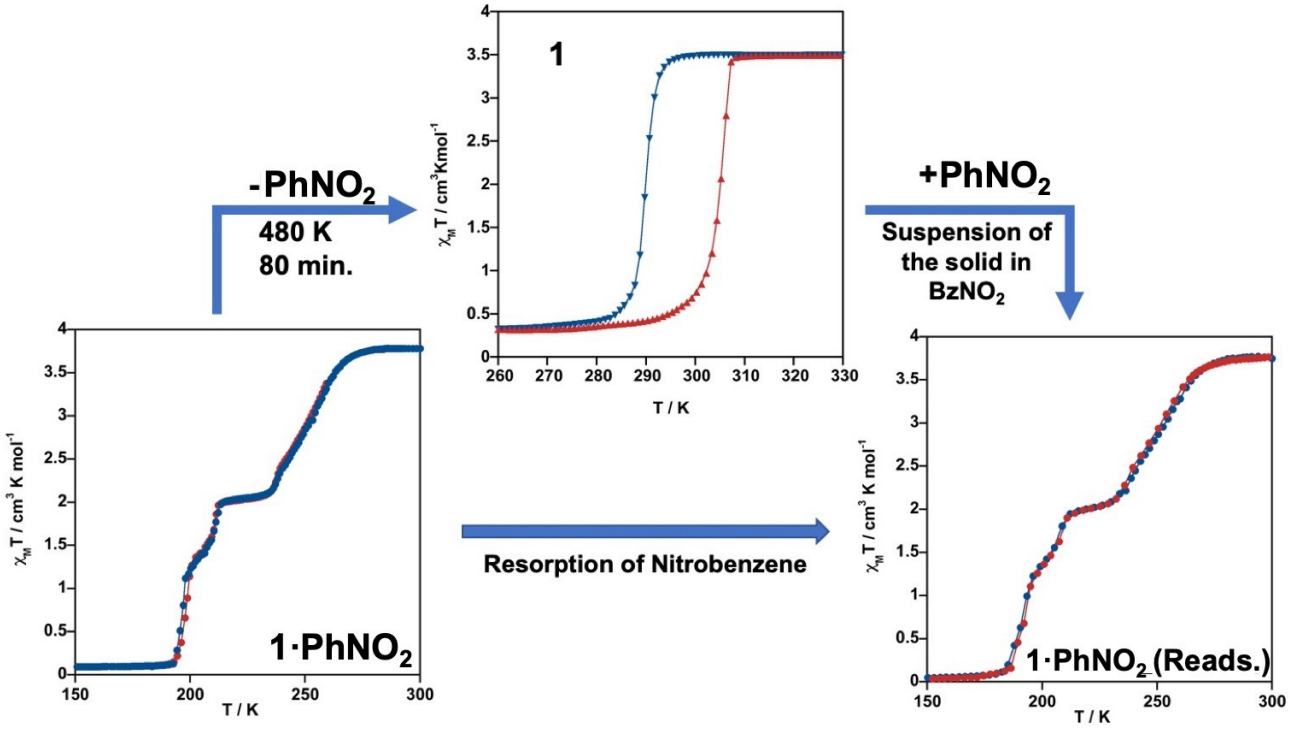

Figure S4. Magnetic properties of **1·PhNO$_2$** emphasising the photo-generation of the metastable HS* states at low temperatures (LIESST effect).

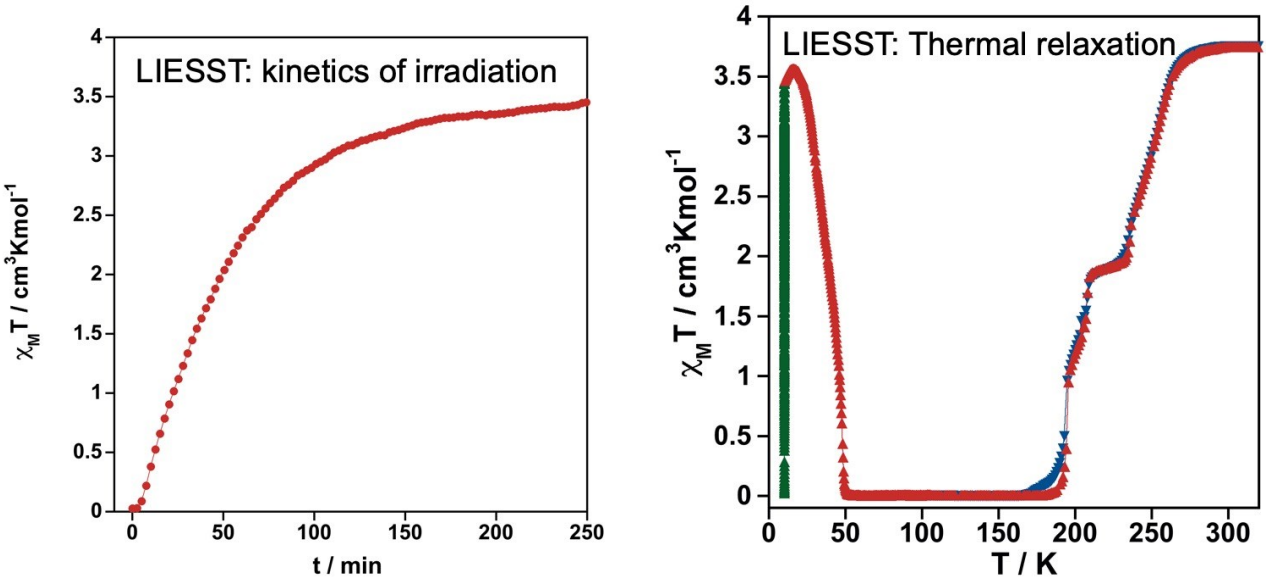

Figure S5. (Left) thermal dependence of $\chi_M T$ (green and blue circles correspond to cooling and heating modes) and ΔH (red line). (Right) thermal dependence of ΔH (red circles) and its derivative (blue). The numbers inserted correspond to the critical temperatures for each step (the calorimetric measurement have been measured at 5 K/min).

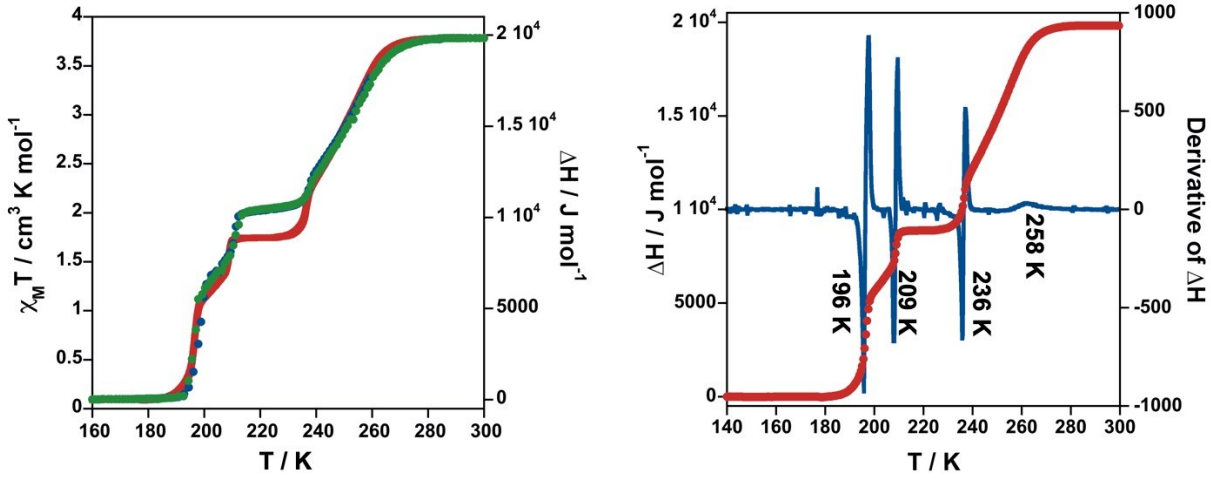

Figure S6. Cell parameters change with temperature and light for **1·PhNO$_2$**.

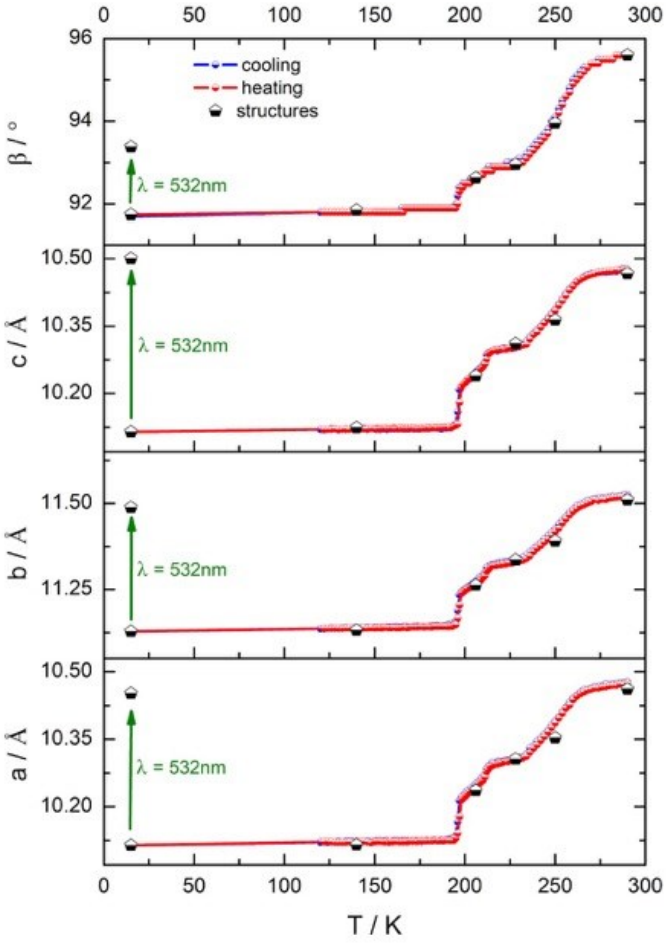

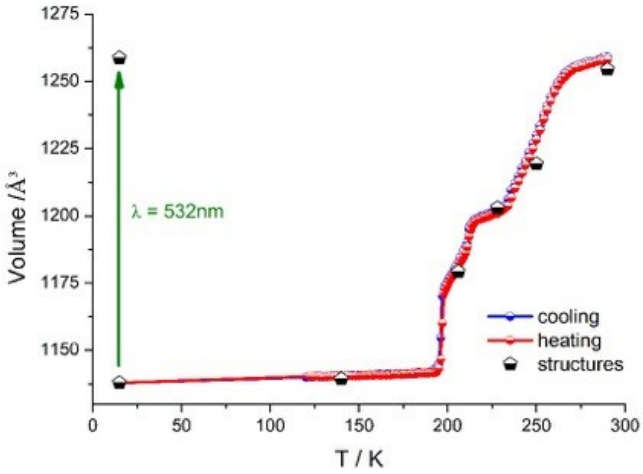

Figure S7. Fragment of one of the two interpenetrated frameworks emphasising the positional disorder of the central ring of the ligand 3,8-phen for **1·PhNO$_2$**.

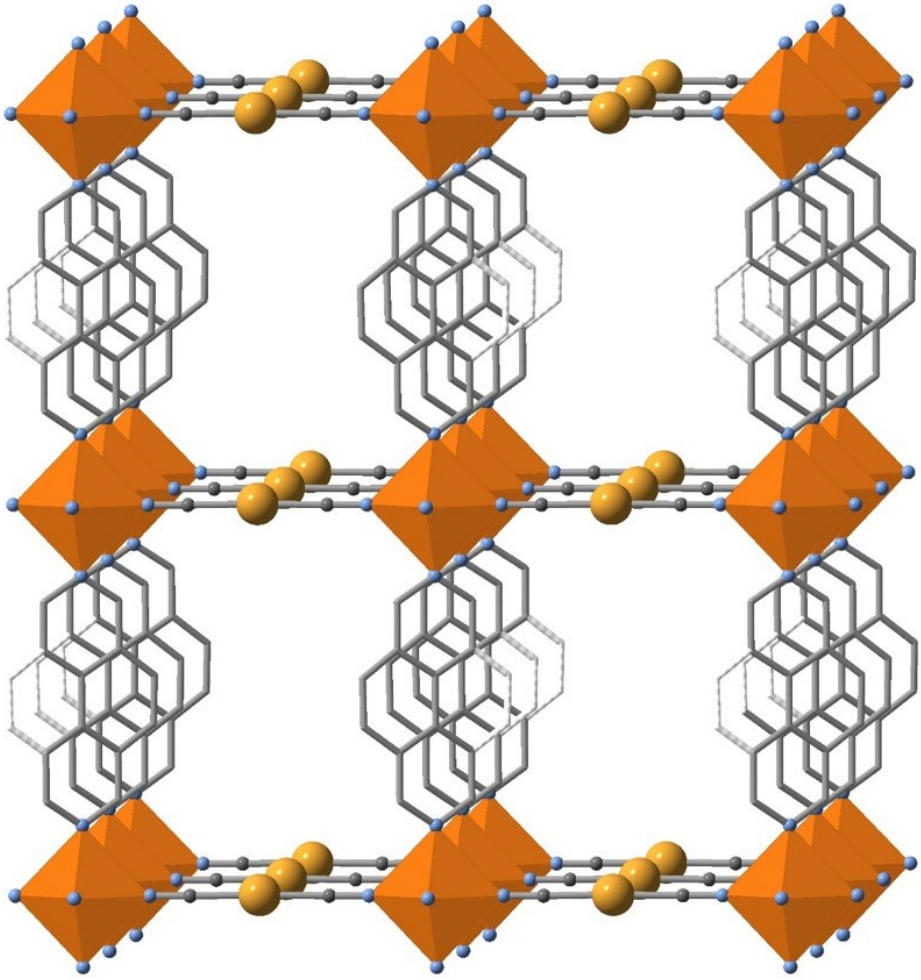

Figure S8. (h0.5l) plane projection with temperature for **1·PhNO$_2$**.

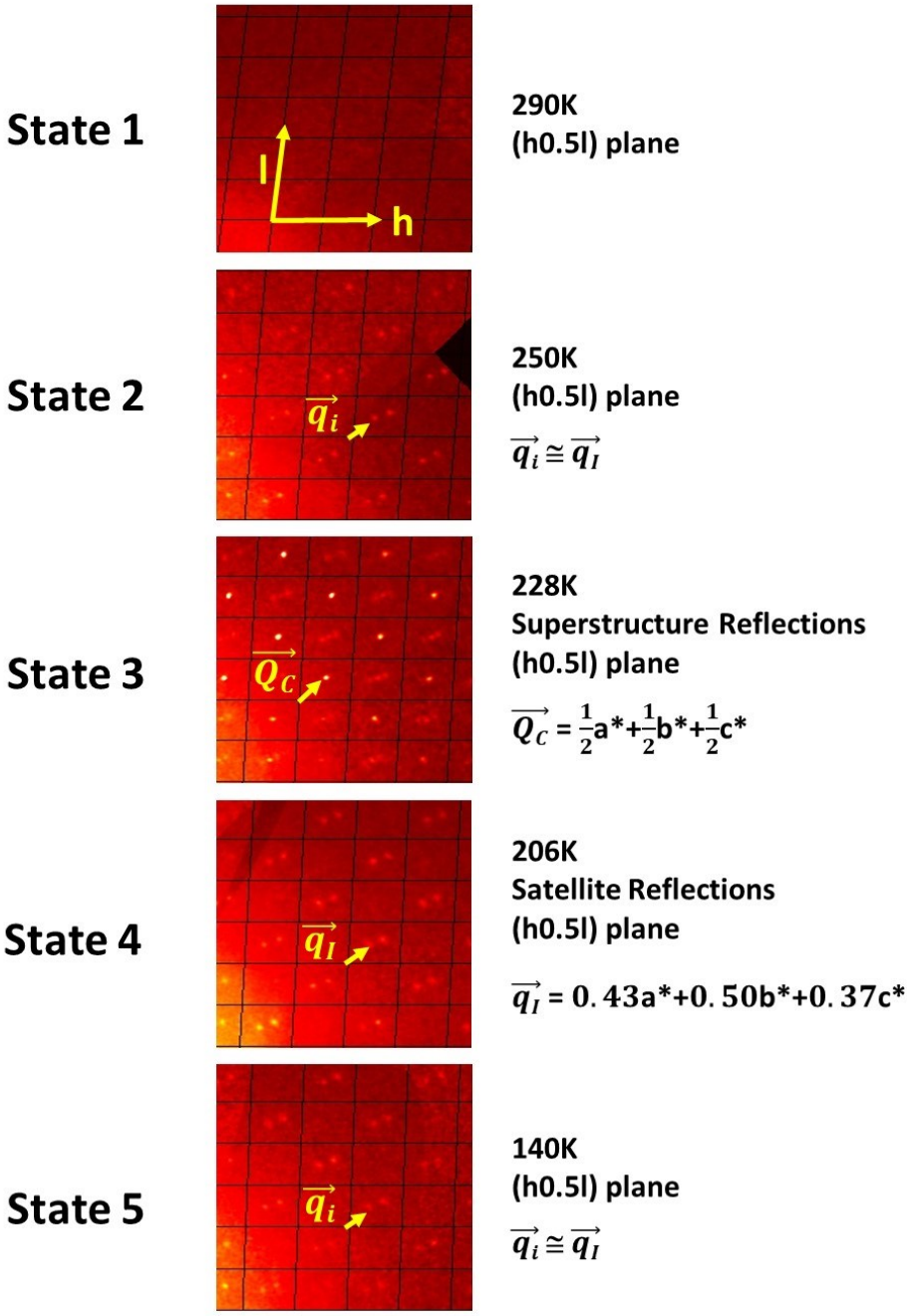

Table S1. Crystal and structure refinement data with temperature and light for **1·PhNO$_2$**.

	State 1	State 2	State 3	State 4	State 5	State 5	State 6/Photo
Temperature/K	290	250.0	228.0	206.0*	140.0	15.0	15.0
Empirical formula	$C_{22}H_{13}Au_2FeN_7O_2$	$C_{22}H_{13}Au_2FeN_7O_2$	$C_{22}H_{13}Au_2FeN_7O_2$	$C_{22}H_{13}Au_2FeN_7O_2$	$C_{22}H_{13}Au_2FeN_7O_2$	$C_{22}H_{13}Au_2FeN_7O_2$	$C_{22}H_{13}Au_2FeN_7O_2$
Formula weight	857.18	857.18	857.18	857.18	857.18	857.18	857.18
Crystal system	monoclinic	monoclinic	monoclinic	monoclinic	monoclinic	monoclinic	monoclinic
Space group	P2/n	P2/n	I2/a	P2/n(a1|2g)0s	P2/n	P2/n	P2/n
a/Å	10.4618(2)	10.3534(3)	14.1982(2)	10.2342(7)	10.1150(2)	10.1143(3)	10.4523(5)
b/Å	11.5106(3)	11.3911(3)	22.6765(3)	11.2690(8)	11.1318(2)	11.1281(3)	11.4885(4)
c/Å	10.4670(2)	10.3639(3)	14.9567(2)	10.2384(7)	10.1239(2)	10.1146(4)	10.5004(4)
β/°	95.605(2)	93.954(3)	90.0258(13)	92.665(5)	91.852(2)	91.745(3)	93.379(4)
Volume/Å^3	1254.43(5)	1219.37(6)	4815.54(12)	1179.51(14)	1139.34(4)	1137.90(6)	1258.71(9)
Z	2	2	8	2	2	2	2
ρ_{calc}g/cm^3	2.269	2.335	2.365	2.4135	2.499	2.502	2.262
μ/mm^{-1}	12.269	12.622	12.784	13.047	13.508	13.525	12.227
F(000)	788.0	788.0	3152.0	788.0	788.0	788.0	788.0
2Θ range for data collection/°	6.34 to 54.0	6.46 to 54.0	6.11 to 54.0	6.02 to 66.4	6.69 to 54.0	5.78 to 54.0	6.69 to 54.0
Reflections collected	22283	10723	39378	40157	9626	5915	8184
Independent reflections	2749 [R_{int} = 0.0401, R_{sigma} = 0.0219]	2675 [R_{int} = 0.0284, R_{sigma} = 0.0252]	5259 [R_{int} = 0.0454, R_{sigma} = 0.0270]	12688(3704+8984) [$R_{(int)}$ = 0.0459, R_{sigma} = 0.0676]	2494 [R_{int} = 0.0293, R_{sigma} = 0.0266]	2490 [R_{int} = 0.0361, R_{sigma} = 0.0547]	2758 [R_{int} = 0.0442, R_{sigma} = 0.0565]
Refinement method	F^2	F^2	F^2	F	F^2	F^2	F^2
Data/restraints/ parameters	2749/45/181	2675/45/180	5259/117/407	12688 / 19 / 394	2494/43/180	2490/92/180	2758/79/180
Goodness-of-fit	1.026	1.061	1.033	$1.55_{(obs)}/1.18_{(all)}$	1.072	1.057	1.074
Final R indexes [I>=2σ (I)]	R_1 = 0.0247, wR_2 = 0.0543	R_1 = 0.0287, wR_2 = 0.0642	R_1 = 0.0300, wR_2 = 0.0691	$R_{1(all)}$ = 0.0416, $wR_{2(all)}$ = 0.0487; $R_{1(main)}$ = 0.0335, $wR_{2(main)}$ = 0.0412; $R_{1(sat)}$ = 0.1093, $wR_{2(sat)}$ = 0.1380	R_1 = 0.0272, wR_2 = 0.0625	R_1 = 0.0370, wR_2 = 0.0808	R_1 = 0.0359, wR_2 = 0.0687
Final R indexes [all data]	R_1 = 0.0324, wR_2 = 0.0571	R_1 = 0.0441, wR_2 = 0.0707	R_1 = 0.0480, wR_2 = 0.0779	$R_{1(all)}$ = 0.1618, $wR_{2(all)}$ = 0.0706; $R_{1(main)}$ = 0.0635, $wR_{2(main)}$ = 0.0467; $R_{1(sat)}$ = 0.4403, $wR_{2(sat)}$ = 0.2400	R_1 = 0.0349, wR_2 = 0.0660	R_1 = 0.0587, wR_2 = 0.0913	R_1 = 0.0548, wR_2 = 0.0775
Largest diff. peak/hole / e Å^{-3}	0.56/-0.45	1.00/-0.82	1.21/-0.81	0.45/-0.58	2.10/-1.35	2.35/-1.03	1.37/-1.11

Figure S9. Rietveld refinement of compound **1**.

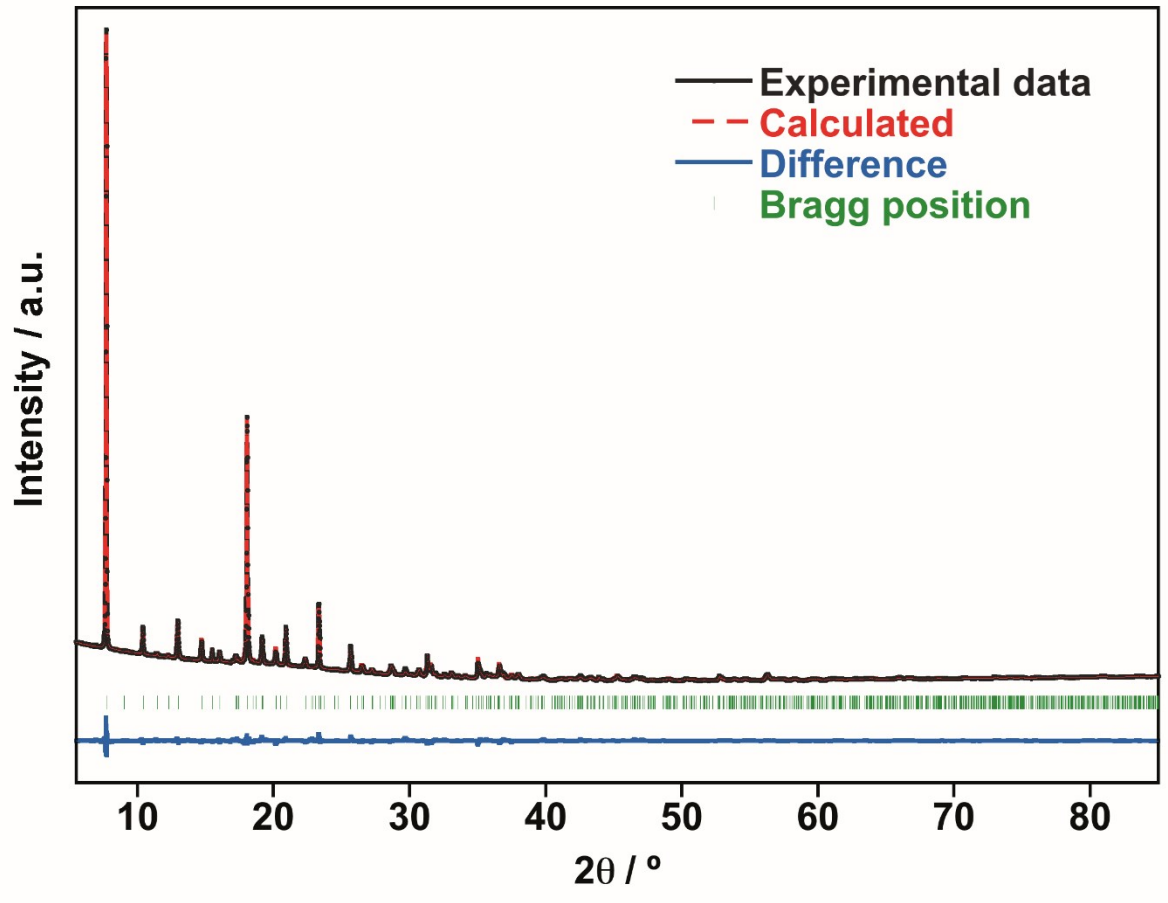

Table S2. Selected crystallographic data from Powder X-ray diffraction of compound **1**.

Temperature/K	290
Empirical formula	C_{16} H_8 Au_2 Fe N_6
Formula weight	734.07
Crystal system	Monoclinic
Space group	*C*2/*m*
a/Å	12.0682(4)
b/Å	16.9687(4)
c/Å	11.4632(3)
β/°	94.888(4)
Volume/Å³	2338.91(11)
Z	4
ρ_{calc}g/cm³	2.08470
Wavelength/ Å	1.540596
pd proc ls prof R factor	2.12
pd proc ls prof wR factor	3.06
pd proc ls prof wR expected	1.48
Refine ls goodness of fit all	2.06
Refine ls R factor all	1.72

Table S3 (left)/Figure S10 (right). Selected bond lengths and angles and a representative fragment of the molecular building blocks of compound **1**. The two possible orientations of the ligand 3,8-phen as well as the positional disorder of C4 and C5 have been omitted for clarity.

Au1-C15	1.999(12)
Au1-C16	1.999(12)
Fe12-N2	2.252(2)
Fe12-N3	2.246(2)
Fe12-N8	2.11(2)
Fe12-N10	2.11(2)
N2-C8	1.333(8)
N2-C9	1.346(7)
N3-C7	1.334(7)
N3-C14	1.243(7)
N8-C15	1.13(2)
N10-C16	1.13(2)
C15-Au1-C16	180.0(6)
N3-Fe12-N10	93.39(11)
N3-Fe12-N8	86.60(11)
N2-Fe12 -N10	86.61(11)
N2-Fe12-N8	93.40(11)
N10-Fe12-N10	94.9(8)
Fe12-N8-C15	168.0(19)
Fe12-N10-C16	168.0(19)

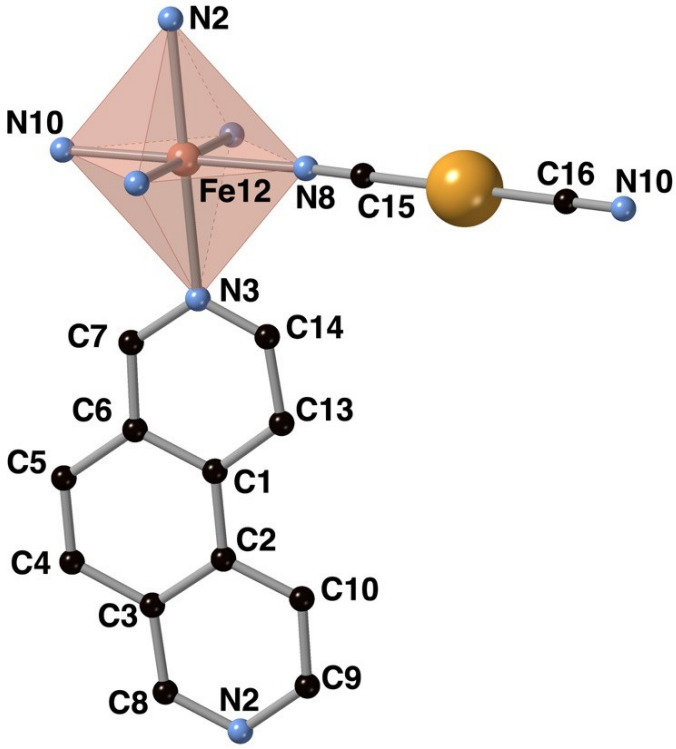

Figure S11. Fragment of one of the two interpenetrated frameworks of **1** showing the two possible orientations of the ligand 3,8-phen and positional disorder of C4 and C5 atoms.

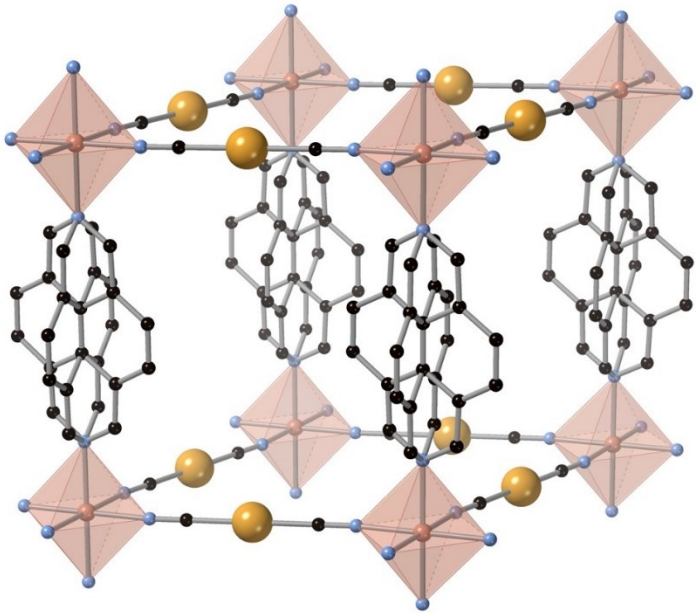

Figure S12. Two orthogonal views of the structure of **1**. The two identical interpenetrated frameworks are coloured in red and blue.